VOLUME ADJUSTABLE TOPOLOGY OPTIMIZATION WITH MULTIPLE DISPLACEMENT CONSTRAINTS

C. W. Huang*

Department of Civil Engineering
Chung Yuan Christian University
Taoyuan, Taiwan

K. W. Chou

National Center for Research on Earthquake Engineering
Taipei, Taiwan

ABSTRACT

Most topology optimization methods seek optimal topologies that satisfy a minimum compliance with a pre-specified volume constraint in the design domain. However, practical designs often include various functional constraints and the optimal solid volume ratios are unknown *a priori*, which implies a gap between topology optimization methods and practical designs in industries. This paper studies the performance-based topology optimization (PTO) problem that searches for the optimal topology with minimum compliance to satisfy the pre-specified functional constraints without a pre-specified volume constraint. A novel element-based evolutionary switching method (ESM), which can automatically adjust solid volume ratio and material distribution, is developed and implemented using the commercial finite element software ABAQUS. The effects of displacement constraints on the optimal topologies are investigated, and the differences between PTO problems and the topology optimization problem which has a volume constraint are discussed. Numerical examples demonstrate that the optimal topologies are mainly determined by the load pattern and locally changed with respect to the location of the active displacement constraints. In addition, the displacement constraints to a large extent control the solid volume ratio of optimal topologies according to the allowable displacements in PTO problems. Finally, the proposed ESM could provide conservative solutions to the topology optimization with multiple displacement constraints problems.

Keywords: Performance-based topology optimization, Functional constraints, Without volume constraints, Evolutionary switching method.

1. INTRODUCTION

Structural optimization is often divided into three types, namely sizing, geometrical, and topology optimization [1]. For sizing and geometrical optimization, the topology of a structure cannot be changed during the optimization process. The structure obtained is thus not guaranteed to be the best, or even good, since another initial topology might produce a much better solution to the optimization problem. However, topology optimization looks for the best topology that satisfies a volume constraint in the design domain. The final optimization solution will therefore be the best of the three solutions obtained from the three types of optimization methods [2].

Topology optimization has recently received intensive attention in both industry and academia due to the rapid developments of sophisticated but inexpensive computers with graphic capabilities, multi-core processors, and high computation speeds. Many methods, such as the homogenization method [3, 4], the power-law approach [5-7], element-based evolutionary methods [8-12], and the level set method [13-15] have been proposed for the topology optimization of continuum structures. The homogenization method is based on the modeling of a porous material constructed with a basic unit cell consisting of a material and a void at a microscopic level. The optimal topology is obtained by continuously varying the distribution of the material. The power-law method assumes that material density within each element used to discretize the design domain is the design variable. The material properties within each element

* Corresponding author (cwhuang@cycu.edu.tw)

DOI : 10.1017/jmech.2017.68
Copyright © 2017 The Society of Theoretical and Applied Mechanics
https://doi.org/10.1017/jmech.2017.68 Published online by Cambridge University Press

are modelled as the relative material densities raised to some power times the material properties of solid material. Element-based evolutionary methods have resulted from fully stressed design techniques; they generate structural topologies by sequentially eliminating or adding elements, depending on the efficiency of each element at each iteration. Level-set methods define the interfaces between material phases implicitly by iso-contours of a level-set function. This implicit function allows a crisp description of the boundaries. In general, the level-set methods consist of three major parts, namely the level-set function parameterization, the mechanical model, and the optimization strategy.

Most continuum-based topology optimization methods can be interpreted as seeking the optimal distribution of a fixed amount of material over a reference domain, using a specified objective function. In general, for a linearly elastic structure, the specified objective function is the minimization of compliance. The compliance of a structure is often defined as twice the work done by the external forces, or the strain energy in the deformed structure, which can be expressed in the following matrix form:

$$\text{Min. } C_p = \mathbf{P}^T \mathbf{U} \tag{1}$$

where **P** and **U** represent the global force and displacement vectors, respectively; C_p denotes the compliance of the structure. Since the displacement vector is the implicit function of design variables, it is obtained by solving the equilibrium equation in the finite element method:

$$\mathbf{KU} = \mathbf{P} \tag{2}$$

where **K** denotes the global stiffness matrix of the structure. Finally, the volume of the material must satisfy the prescribed volume limit $(V)_{specified}$.

$$V \le (V)_{specified} \tag{3}$$

However, with respect to developing practical engineering designs, the mathematical model for the topology optimization problem that has a pre-specified volume constraint falls short in several ways. First, there are no functional constraints, such as displacement, stress, or natural frequency constraints, in such topology optimization problems. A structure with no functional constraints indeed does not satisfy the requirements of practical applications. Second, from the viewpoint of a designer, the "optimal value" of the solid volume fraction in the design space is usually unknown *a priori*. The prescribed volume limits $(V)_{specified}$ in practical design procedures are thus often criticized and appear to violate common senses.

In considering functional constraints, Chu *et al.* [16-17] derived a sensitivity number on nodal displacement to measure the efficiency of each element under the prescribed displacement constraint in the evolutionary structural optimization method. To examine frequency constraints in topology optimization, Zhao *et al.* [18] developed a sensitivity number for natural frequency. However, the definitions of the objective functions become unclear when the sensitivity number is used as the criterion for removing elements in the evolutionary process. Bendsøe and Sigmund [19] investigated topology optimization of compliant mechanisms for geometrically nonlinear structures. Local displacement constraints were placed in the optimization via the objective function rather than via the constraints formulation. Huang and Xie [20] extended the bidirectional evolutionary structural optimization method (BESO) into stiffness optimization with a material volume constraint and a local displacement constraint. A Lagrangian multiplier was introduced into the topology optimization formulation. Lin and Hsu [21-22] proposed an adaptive volume constraint algorithm in density-based methods, to facilitate searching for a minimum compliance design that simultaneously satisfies additional displacement or stress constraints.

Nevertheless, the relationships between optimal topologies and their constraints, including volume and functional constraints, have not been well discussed. Theoretically speaking, functional and volume constraints are generally competitive in topology optimization for continuum structures. There is no guarantee that the functional constraints will be satisfied under a pre-specified volume constraint (details are discussed in Section 3). For instance, it is impossible to satisfy a smaller allowable displacement constraint with a larger material removal ratio. As a result, a performance-based topology optimization (PTO) problem is investigated in this paper. In PTO problems, the objective function is defined as minimizing the compliance of a linearly elastic structure. On the other hand, the volume constraint is removed, but functional constraints are added. The differences between the topology optimization with the volume constraint and the performance-based topology optimization problems are discussed through numerical examples in the following.

The remainder of this paper is organized as follows. In Section 2, the mathematical model used for the PTO problem is defined. Then a novel evolutionary switching method (ESM) which can automatically adjust solid volume ratio and material distributions is proposed. The proposed ESM is an element-based method and combines the characteristics of the evolutionary structural optimization (ESO) method and element exchange method (EEM). In Section 3, three design examples are presented to study the effects of functional constraints on optimal topologies. The physical interpretations of the results for PTO problems are discussed in this section. Conclusions are summarized in Section 4.

2. METHODOLOGY

The mathematical model corresponding to the PTO problem can be written as follows:

$$\text{Min. } C_p = \mathbf{P}^T \mathbf{U} \tag{4a}$$

$$\text{Sb. } g_j(\mathbf{u}) \le (g_j)_{allow} \quad j = 1, 2, \ldots, n \tag{4b}$$

$$\mathbf{KU} = \mathbf{P} \tag{4c}$$

where **u** represents the nodal displacement vector and

https://doi.org/10.1017/jmech.2017.68 Published online by Cambridge University Press

$(g_j)_{allow}$ denotes the allowable values of the j^{th} functional constraint. The PTO problem thus focuses on structural performance (such as displacements and stresses) in practical situations, requiring that the optimized topology is coupled with minimum compliance.

For a structure discretized using finite elements, PTO aims to determine the optimal distribution of solid and void elements that would satisfy Eq. (4). To achieve the objective function of compliance minimization, element strain energy is used as the main criterion for element adjustment. An evolutionary switching method (ESM) is proposed to solve PTO problems that consider functional constraints. This method is a double-loop optimization algorithm, comprising an outer loop and an inner loop. The outer loop (evolutionary loop) adjusts the volume of materials to satisfy the functional constraints. The inner loop (switching loop) identifies the optimal topology for a specified volume of material, which is determined by the evolutionary loop. More details of the ESM are discussed in the following sections.

2.1 Evolutionary Loop

In the PTO problem, the optimal solid element volume in the design domain is unknown *a priori*. The evolutionary loop adjusts the volume of the solid element from the volume of the initial topology $(V_s)_{initial}$ to a trial target solid element volume $(V_s)_{target}$. The latter is a candidate for the optimal solid element volume. If $(V_s)_{initial}$ is equal to $(V_s)_{target}$, then the evolutionary loop is omitted and the ESM verifies whether the candidate qualifies as optimal in the switching loop (see Section 2.3 for more details).

To reach $(V_s)_{target}$, the evolutionary loop gradually adjusts the solid volume by replacing solid elements with void ones or vice versa until $(V_s)_{initial}$ is equal to $(V_s)_{target}$. The concept of the evolutionary loop originates from the evolutionary structural optimization (ESO) method [9]. When $(V_s)_{initial}$ is not equal to $(V_s)_{target}$, a finite element analysis (FEA) is performed to compute the strain energy of each element. If $(V_s)_{initial}$ is smaller than $(V_s)_{target}$, a subset of void elements with higher strain energies is converted into solid elements. If $(V_s)_{initial}$ is larger than $(V_s)_{target}$, a subset of solid elements with lower strain energies is converted into void elements. A characteristic feature of the evolutionary loop is the commutability of the material properties of the elements. An element, depending on its strain energy, can be converted from a solid to a void in one iteration and back to a solid in a subsequent iteration.

In summary, a number of elements are converted, according to their strain energy, at each iteration. Then an FEA is performed on the modified topology model to update element strain energies for the next iteration, until the solid volume equals $(V_s)_{target}$ in the evolutionary loop. The number of converted elements is not necessarily minimized, but should be small enough that the evolutionary loop can create a topology that is not too far from the optimal. A smaller value of M_e would result in a more accurately developed topology which more approaches the optimal topology and decreases the number of iteration in the switching loop, but the smaller value of M_e would increase the number of iteration in the evolutionary loop. On the other hand, a larger value of M_e would result in a poor topology which may be different from the optimal topology and increases the number of iteration in the switching loop, but the larger value of M_e would decrease the number of iteration in the evolutionary loop. Basically speaking, how many elements an evolutionary iteration should convert, M_e, might result from a compromise between computational accuracy and efficiency. In this paper, the number of elements converted in each evolutionary iteration (M_e) is constrained to be 1% of the solid element count for the previous trial volume.

2.2 Switching Loop

For a trial $(V_s)_{target}$, the switching loop exchanges elements to determine the optimal topology of a structure that achieves minimum compliance without changing the volume of the solid elements. Which elements are converted is determined by two switching policies, namely the sorting switch and the random switch.

Using the sorting switch, a subset of solid elements with lower strain energy is converted into void elements, and an equal size subset of void elements with higher strain energy is converted into solid elements. Numerical experience shows that the number of elements exchanged at each iteration of the sorting switch (M_s) should be larger at the beginning of the switching loop, to speed up the optimization process, and decrease towards the end of the loop, to avoid missing a better topology. Therefore, the suggested formula for M_s is proposed as follows:

$$(M_s)_{(k)} = \text{int}[a \cdot Exp(b \cdot (k-1)^{\lambda})] \quad \text{for } k = 1, 2, \ldots, N_{s-\max} \tag{5}$$

where

$$a = M_{s-\max} \tag{6a}$$

$$b = \frac{\ln(M_{s-\min}) - \ln(M_{s-\max})}{(N_{s-\max})^{\lambda}} \tag{6b}$$

and int[·] denotes the Gaussian symbol, k is iteration number; λ is the parameter that controls the rate of convergence (0.75 in this study), and $N_{s\text{-max}}$ is the iteration number maximum. In addition, $M_{s-\max}$ is the maximum number of exchanged element in the first iteration ($k = 1$) and $M_{s-\min}$ denotes the minimum number of exchanged element in the final iteration ($k = N_{s\text{-max}}$). Since the evolutionary loop is intended to prepare a near-optimal topology, $N_{s\text{-max}}$ is set to 100 in this paper. In addition, $M_{s-\max}$ and $M_{s-\min}$ are set to 3% and 0.2% of the number of solid elements, respectively, to obtain a better topology according to our numerical experiences.

Theoretically speaking, the sorting switch is equivalent to the simplex method if $M_s = 1$ (the derivation is shown in the Appendix). The objective function, i.e. compliance, decreases monotonically with repetition of the sorting switch, and the optimal topology is obtained when the objective function has been minimized. How-

https://doi.org/10.1017/jmech.2017.68 Published online by Cambridge University Press

ever, if $M_s \neq 1$, there is no guarantee that sequentially exchanging elements brings out the optimal topology. The random switch [12] is therefore introduced to enhance the likelihood of obtaining a better solution and to avoid identifying local optima in topology optimization problems.

In the random switch, two sets containing the same number of elements are randomly selected. One is a subset of solid elements and the other is a subset of void elements. The solid subset then becomes void, and vice versa. This procedure is similar to mutation in a genetic algorithm (GA), which randomly distributes solid elements throughout the void regions to explore the design space more widely. The number of elements participating in the random switch, M_r, is determined using a decreasing linear function as follows [12]:

$$(M_r)_{(k)} = \text{int}\left[M_{r-\max} - k\left(\frac{M_{r-\max} - M_{r-\min}}{N_{s-\max}} \right) \right]$$
$$\text{for } k = 1, 2, \ldots, N_{s-\max} \tag{7}$$

For convenience, $M_{r\text{–max}}$ and $M_{r\text{–min}}$ can be set equal to $M_{s\text{–max}}$ and $M_{s\text{–min}}$. It is important to note that although the random switch may prevent premature convergence, it disrupts the convergence of the objective function. As a result, the random switch is only triggered under three conditions: (1) the value of the current objective function increases by 2% of the previous iteration; (2) the value of the objective function varies between two values for two successive iterations; and (3) the switching iteration number is a multiple of the return period of the random switch. In this paper, the return period is 20 iterations.

The switching loop continues until its iteration number reaches the greatest iteration number $N_{s\text{-max}}$, or the compliance variance between two successive iterations is less than the predefined tolerance e_C, as follows:

$$\left| \frac{(C_p)_{(k)} - (C_p)_{(k+1)}}{(C_p)_{(k+1)}} \right| \leq e_C \tag{8}$$

where the subscripts in parentheses represents the iteration number. The allowable tolerance e_C is set as 10^{-3} in this study.

2.3 Volume Adjustment

The switching loop determines the optimal topology for $(V_s)_{target}$. The functional constraints of the optimal topology are evaluated according to the FEA. For simplicity, only the displacement constraints are discussed in this paper. When the displacement constraints are not satisfied, this implies that $(V_s)_{target}$ is incorrect and needs to be adjusted. For PTO problems with multiple displacement constraints, Eq. (9) is used to adjust the initial solid element volume and trial target solid element volume for the next iteration of the evolutionary loop:

$$(V_s)_{initial}^{(i+1)} = (V_s)_{target}^{(i)} \tag{9a}$$

$$(V_s)_{target}^{(i+1)} = (V_s)_{target}^{(i)} \times R_V^{(i)} \tag{9b}$$

$$R_V^{(i)} = \max\left(\frac{u_j}{(u_j)_{allow}} \right) \tag{9c}$$

where the superscript in the parentheses denotes the execution number of the evolutionary loop that adjusts the volume. The terms u_j and $(u_j)_{allow}$ represent the j^{th} displacement and the corresponding allowable displacement, respectively. Equation (9c) implies that $(V_s)_{target}$ is controlled by the displacement constraint that has the maximal ratio of the displacement to its allowable value among all displacement constraints. Such a controlling constraint is considered active in this paper.

The ESM is completed when the displacement value for the active constraint satisfies the following convergence criterion:

$$\left| \frac{u_j - (u_j)_{allow}}{(u_j)_{allow}} \right| \leq e_u \tag{10}$$

where e_u denotes the predefined convergence tolerance, which is set as 10^{-2} in this paper.

2.4 ESM Algorithm and Implementation

The procedure of the ESM is summarized as follows and depicted in Fig. 1.

Step 1. Discretize the design domain into finite element meshes and set the initial topology for the initial solid volume $(V_s)_{initial}$. For convenience, the first trial target solid volume $(V_s)_{target}$ can be set equal to $(V_s)_{initial}$.

Step 2. Proceed to Step 6 if the current solid element volume reaches $(V_s)_{target}$.

Step 3. If the current solid element volume has not reached $(V_s)_{target}$, analyze the finite element model for the given loads, compute the strain energies for all elements, and smooth the strain energies for all elements to avoid a checkerboard pattern [23].

Step 4. Sort the solid and void elements, respectively, in descending order according to their smoothed strain energies.

Step 5. Adjust the solid element volume by either increasing or decreasing solid elements. The number of elements converted at each evolutionary iteration is M_e. Return to Step 2.

Step 6. Enter the switching loop to identify the optimal topology under $(V_s)_{target}$: analyze the finite element model for the given loads, compute the strain energies for all elements, and smooth the strain energies for all elements to avoid a checkerboard pattern [23].

Step 7. Sort the solid and void elements, respectively, in descending order according to their smoothed strain energies.

Step 8. Compute the number of solid elements to be exchanged at each switching iteration, according to Eq. (5). Perform the sorting switch for solid and void element sets without changing the solid volume. Moreover, perform the random switch

https://doi.org/10.1017/jmech.2017.68 Published online by Cambridge University Press

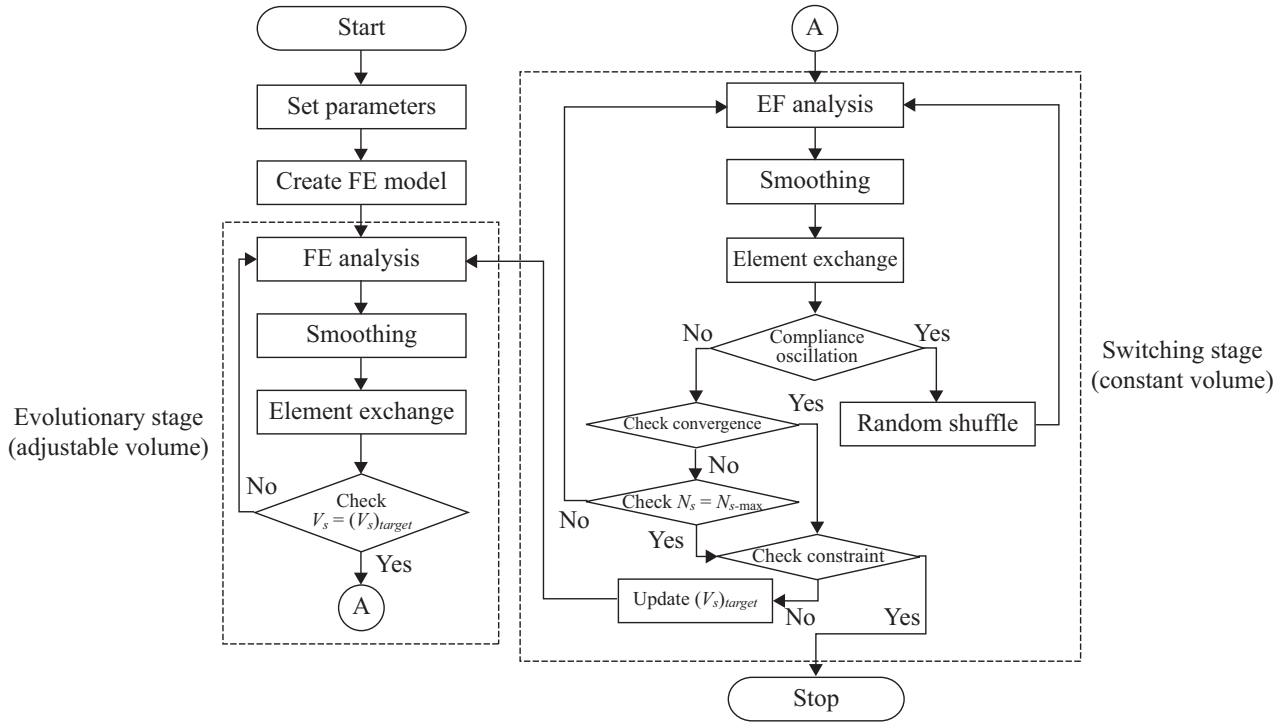


Fig. 1 Flowchart of the proposed evolutionary switching method.

if any of the three conditions mentioned in Section 2.2 are encountered.

Step 9. Evaluate Eq. (8) to check whether the compliance converges. Proceed Step 10 if the compliance converges or the iteration number of the switching loop N_s has reached the predefined maximum iteration number. Otherwise, return to Step 6.

Step 10. Find the controlling displacement constraint that gets the maximum ratio of displacement to allowable displacement among all constraints. Check whether the controlling displacement constraint satisfies Eq. (10). If not, update $(V_s)_{target}$ according to Eq. (9) and return to Step 2. Otherwise, the ESM is completed.

It is worth noting that the proposed ESM can also be used to solve the topology optimization problem which has a volume constraint. To do this, users must set $(V_s)_{target}$ equal to $(V)_{specified}$ and stop the optimization process after Step 9. The proposed ESM is implemented with the commercial finite element software, ABAQUS [24], to ensure that it can obtain reliable finite element analyses. The computational framework was developed in the programming language Python, because ABAQUS/CAE offers a Python application programming interface (API) for the user to construct interactive designs [25]. Through the ABAQUS Python API, the ESM can conduct ABAQUS FEAs, access the ABAQUS output database, modify the finite element model, and display the evolving topologies in the ABAQUS/CAE viewport. Figure 2 shows the architecture of our ESM program in unified modeling language (UML).

3. NUMERICAL EXAMPLES

In this section, the proposed ESM is used to minimize the compliance of the structure with displacement constraints. To prevent ill-conditioning of the stiffness matrix, the void elements are assumed to have very small elastic moduli, i.e. $E_{void} = 10^{-4} E_{solid}$. In addition, Poisson's ratio, ν, for both materials is 0.3. The initial solid volume $(V_s)_{initial}$ and initial trial target solid volume $(V_s)_{target}$ are both assumed to be in the fully filled design domain. Linear elastic static analyses are performed using ABAQUS to compute the strain energy of each element.

3.1 Example 1

The first example is a two-dimensional beam structure which is supported at both ends. A vertical load (P = 100 N) is applied in the middle of the upper edge (Fig. 3) [20]. Because of the symmetry of the structure, only the right half of the design domain is analyzed. This half is discretized into 100 × 100 quadratic plane stress elements (CPS8 in ABAQUS), each with an area of 0.5 × 0.5 mm. The elastic modulus for solid elements, E_{solid}, is 1 GPa. For the purpose of comparison, a topology optimization with a volume constraint problem in which no displacement constraint is defined and the volume constraint is 30% of the design domain is considered firstly. Figures 4(a) and (b) illustrate the optimal topologies produced by the ESM and BESO [20], respectively. The skeleton of the optimal topology obtained from the ESM is similar to that produced by BESO, except for the angle of the compression struts in the middle part of the beam. The differences in optimal topologies

https://doi.org/10.1017/jmech.2017.68 Published online by Cambridge University Press

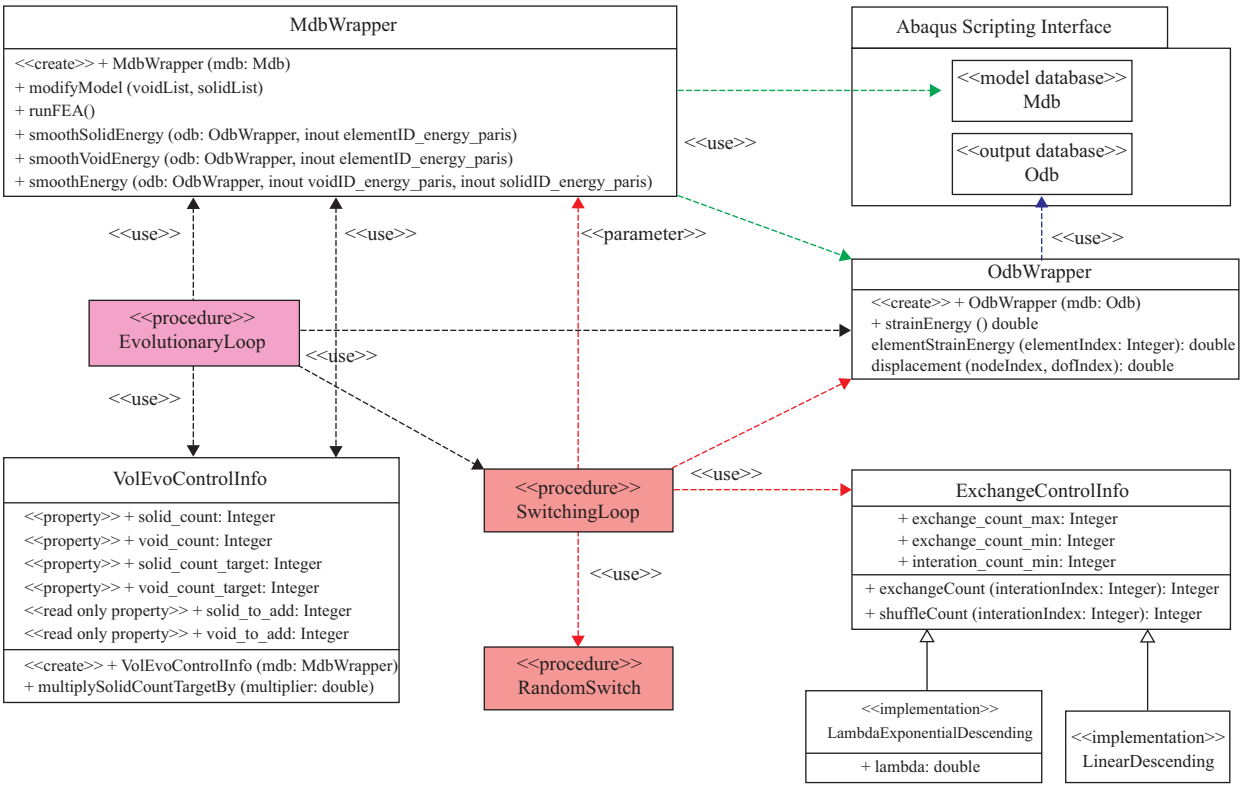


Fig. 2 UML of the developed Python program for ESM.

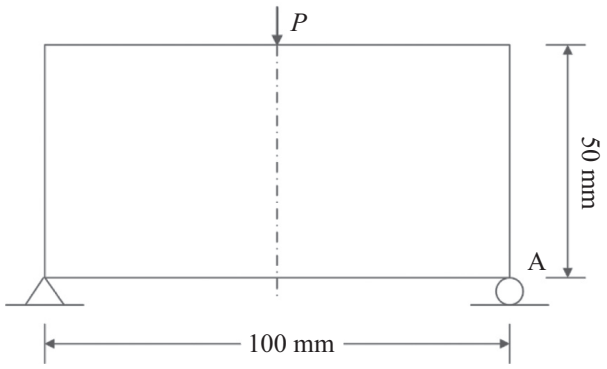
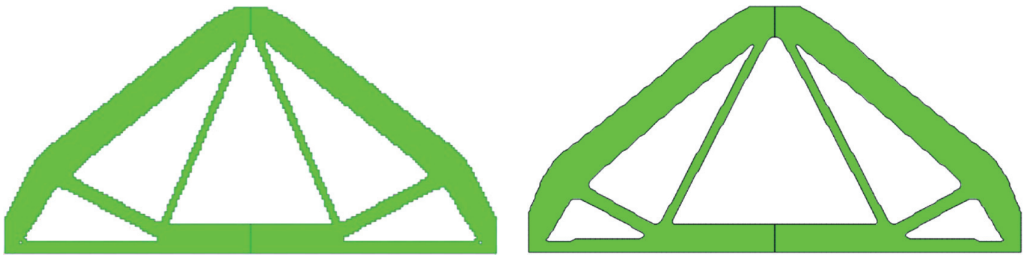


Fig. 3 Design domain and boundary conditions of Example 1.



(a) ESM (b) BESO

Fig. 4 Optimal topologies for Example 1 with solid volume ratio = 30 % from (a) ESM and (b) BESO [20].

https://doi.org/10.1017/jmech.2017.68 Published online by Cambridge University Press

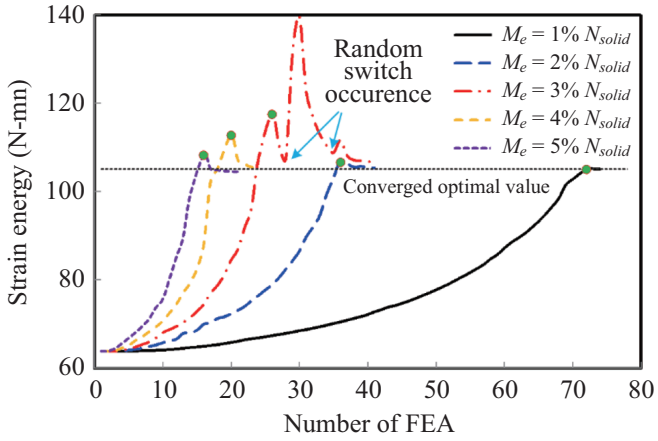


Fig. 5 The history curves of the strain energy versus the number of FEA under different converted element numbers.

Table 1 Strain energy, solid volume ratio, and displacement of optimal topologies in Example 1

Displacement constraints	Strain energy (N-mm)	Volume (%)	Final u_A (mm)
Without disp. constraint	105.12	30.0	0.788
$(u_A)_{allow}$ = 0.6 mm	74.88	55.2	0.595
$(u_A)_{allow}$ = 1.0 mm	141.10	20.4	0.999

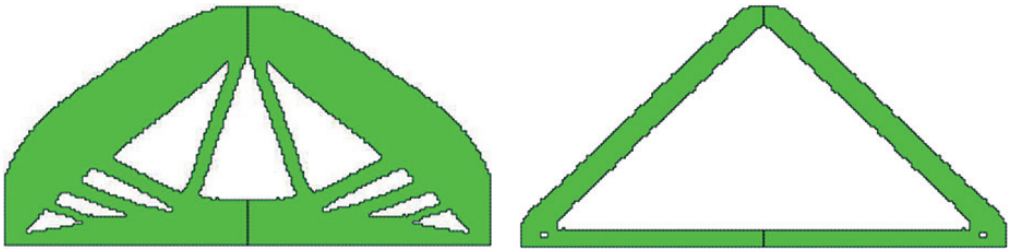
may result from that different types of elements (CPS8 and CPS4) are adopted in the finite element models.

Figure 5 illustrates that the relationships between strain energy and the number of FEAs using the ESM with different values of M_e. In Fig. 5, the green circles and the black dotted line represent the end of the evolutionary loop and the converged optimal strain energy, respectively. It can be seen that larger values of M_e speed up the evolutionary loop linearly; however, the topology identified at the end of the evolutionary loop may not be good enough, and more iterations of the switching loop are required. The abrupt increases in strain energy during the switching loop indicate the times when the random switch was invoked. All cases converge to nearly the same strain energy value (Fig. 5), which implies that the proposed ESM is a robust, stable, and efficient method that is capable of identifying the optimal topology at the end of the switching loop.

The corresponding strain energy and the horizontal displacement of the roller support (point A in Fig. 3) in the optimal topology of Fig. 4(a) are listed in Table 1. The horizontal displacement at point A is 0.788 mm that represents the minimum value of the horizontal displacement at point A under the volume constraint. The result implies that one cannot find another topology which has a horizontal displacement at point A smaller than 0.788 mm under the volume constraint. Moreover, the topology which has a horizontal displacement at point A larger than 0.788 mm under the volume constraint must not be the optimal topology with minimum compliance. As a result, the optimal topologies cannot be obtained if an inappropriate functional constraint is added to the topology optimization problem with a volume constraint. In other words, the volume constraint and the functional constraint are competitive in the topology optimization problems. Except for some well-designed problems with appropriate upper bound on the volume constraint and allowable values of functional constraints in the literature, these two kinds of constraints should not coexist in the topology optimization problems. In addition, once the optimal topology satisfied both with the volume and functional constraints, the compliance will increase because the compliance has more limitations in the design space.

The effects of displacement constraints on optimal topologies are investigated in solving PTO problems. The horizontal displacement of the roller support is considered as the monitored target. The allowable displacements are set to 0.6 mm and 1.0 mm for comparison in this PTO problem. Figures 6(a) and 6(b) are the optimal topologies corresponding to allowable displacements of 0.6 mm and 1.0 mm, respectively, using the proposed ESM without considering volume constraints. It is expected that the solid volume of the optimal topology should increase when the allowable displacement of the roller support, $(u_A)_{allow}$, decreases to resist the given loadings. Comparing Fig. 4(a) with Fig. 6, one can see that only the outer skeletons are similar, and that the inner members of the optimal topologies are distinctly different. For a smaller $(u_A)_{allow}$, more inner tension members are generated to decrease the horizontal displacement of the roller support. In contrast, for a larger $(u_A)_{allow}$ the inner members are removed from the original optimal topology and the external loading is transferred to the end supports directly. The strain energies, final solid volume ratios, and the horizontal displacement of

https://doi.org/10.1017/jmech.2017.68 Published online by Cambridge University Press



(a) $(u_A)_{allow}$ = 0.6 mm (b) $(u_A)_{allow}$ = 1.0 mm

Fig. 6 Optimal topologies of Example 1 with minimum compliance and a horizontal displacement constraint at the roller support without considering the volume constraint (a) $(u_A)_{allow}$ = 0.6 mm and (b) $(u_A)_{allow}$ = 1.0 mm.

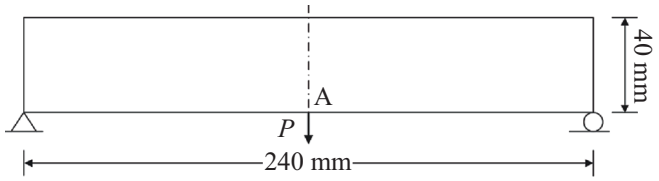
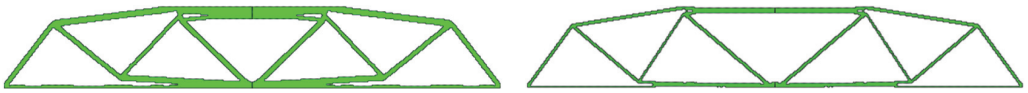


Fig. 7 Design domain and boundary conditions of Example 2.



(a) $(u_A)_{allow}$ = 0.2 mm (b) $(u_A)_{allow}$ = 0.4 mm

Fig. 8 Optimal topologies of Example 2 with minimum compliance and a vertical displacement constraint at the middle point from ESM without considering the volume constraint (a) $(u_A)_{allow}$ = 0.2 mm and (b) $(u_A)_{allow}$ = 0.4 mm.

Table 2 Strain energy, solid volume ratio, and displacement of optimal topologies in Example 2

Displacement constraints	Strain energy (N-mm)	Volume (%)	Final u_A (mm)
$(u_A)_{allow}$ = 0.2 mm	10.00	22.0	0.200
$(u_A)_{allow}$ = 0.4 mm	20.02	11.3	0.400

the roller support for the topologies which are illustrated in Fig. 6 are listed in Table 1. These data show that the ESM can be guaranteed to identify the optimal topology that satisfies specified displacement constraints with minimum strain energy.

3.2 Example 2

The second example considers a two-dimensional slender beam that is supported at both ends and vertically loaded (P = 100 N) at the middle of the lower edge (Fig. 7) [26]. Because this design is symmetrical, we analyze only the right half of the design domain. This half is discretized into 80 × 240 quadratic plane stress elements (CPS8 in ABAQUS), each with an area of 0.5 × 0.5 mm. The elastic modulus for solid elements, E_{solid}, is 100 GPa. It is required that the vertical deflection of the middle of the beam should not exceed 0.2 mm or 0.4 mm, respectively, as two allowable displacement values.

The optimal topologies corresponding to these two allowable displacements (0.2 and 0.4 mm) are shown in Figs. 8(a) and 8(b), respectively. The strain energies, final solid volume ratios, and vertical displacement of the mid-point of the optimal topologies are listed in Table 2. These data show that the optimal topologies from ESM indeed satisfy the displacement constraints. Comparing Fig. 8(a) with Fig. 8(b), one can see that the outer skeletons of these two optimal topologies are similar. The reason comes from that both optimal topologies have minimum compliance corresponding to the same loadings. In addition, the larger allowable displacement generates the optimal topology which has smaller solid volume ratio. These phenomena imply that the purpose of the displacement constraint is to force the optimization algorithm to identify the optimal solid volume ratio that just satisfies the allowable displacement condition.

https://doi.org/10.1017/jmech.2017.68 Published online by Cambridge University Press

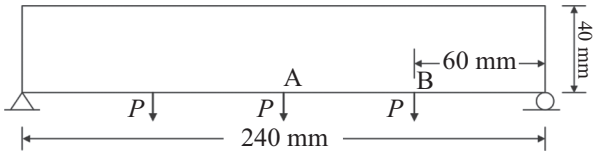
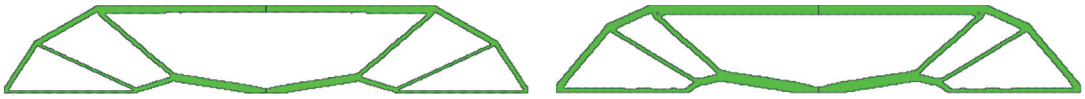


Fig. 9 Design domain and boundary conditions of Example 3.



(a) $(u_A)_{allow}$ = 0.2 mm, $(u_B)_{allow}$ = 0.15 mm (b) $(u_A)_{allow}$ = 0.2 mm, $(u_B)_{allow}$ = 0.1 mm

Fig. 10 Optimal topologies of Example 3 with minimum compliance and two vertical displacement constraint at the middle and quarter points from ESM without considering the volume constraint (a) $(u_A)_{allow}$ = 0.2 mm, $(u_B)_{allow}$ = 0.15 mm and (b) $(u_A)_{allow}$ = 0.2 mm, $(u_B)_{allow}$ = 0.1 mm.

Table 3 Strain energy, solid volume ratio, and displacement of optimal topologies in Example 3

Displacement constraints	Strain energy (N-mm)	Volume (%)	Final u_A (mm)	Final u_B (mm)
$(u_A)_{allow}$ = 0.20 mm $(u_B)_{allow}$ = 0.15 mm	6.684	15.9	0.200	0.123
$(u_A)_{allow}$ = 0.20 mm $(u_B)_{allow}$ = 0.10 mm	5.449	19.9	0.162	0.101

3.3 Example 3

In the third example, the material properties, boundary conditions, geometries, and mesh are the same as those used in the second example. Three concentrated loads (P = 30 N) are applied at the bottom of the beam (Fig. 9). One load is applied at the middle, and the remaining two are applied at a quarter of the way from each end of the beam. Three displacement constraints are specified at the middle and at two quarter points, respectively, to test the ESM under multiple displacement constraints. Figure 10(a) presents the minimum compliance topology which is identified by the proposed ESM for the allowable displacement values of 0.2 mm and 0.15 mm at points A and B (Table 3 denoted these allowable values as $(u_A)_{allow}$ and $(u_B)_{allow}$), respectively. In addition, Fig. 10(b) shows the minimum compliance topology from ESM for $(u_A)_{allow}$ = 0.2 mm and $(u_B)_{allow}$ = 0.1 mm.

Figures 10(a) and 10(b) show similar topologies, with some local differences: the inner oblique tension members are steeper and closer to the quarter point in Fig. 10(b) than in Fig. 10(a); and the member widths in Fig. 10(b) are larger than those in Fig. 10(a). The final strain energies, solid volume ratios, and vertical displacement at points A and B of the optimal topologies are listed in Table 3. From these data, one can see that (u_A) is active in the first case and that (u_B) is active in the second case. The location of the active constraint results in the difference between the two optimal topologies. In Fig. 10(b) the assemblage of solid elements near the bottom quarter point is greater than in Fig. 10(a). The topological difference makes the displacement at point B in Fig. 10(b) smaller than that in Fig. 10(a). Furthermore, comparing Figs. 8(a) with 10(a), one can see that the optimal topology in Example 2 is different from that in Example 3, even though these two examples have the same active displacement constraint at the same point. Such topological differences indicate that displacement constraints are not the main factors to determine optimal topologies. On the other hand, the load pattern dominates the development of the optimal topologyies in PTO problems. This example demonstrates that the proposed ESM can indeed identify optimal topologies under multiple displacement constraints with minimum compliance.

4. CONCLUSIONS

Compared with the topology optimization problem with a volume constraint, the performance-based topology optimization problem is closer to practical design applications. Engineers need only specify the functional requirements, and the material volume ratio is adjusted automatically to achieve minimum compliance with these requirements. The physical meaning of the performance-based topology optimization can be interpreted as what amount materials could be saved under the specified functional constraints with minimum compliance.

In this study, an evolutionary switching method

https://doi.org/10.1017/jmech.2017.68 Published online by Cambridge University Press

(ESM) is proposed to solve performance-based topology optimization (PTO) problems. The novel element-based ESM combined the characteristics of the evolutionary structural optimization (ESO) method and element exchange method (EEM) to adjust the material volume to the displacement constraints. Briefly, an ESM is a double-loop algorithm in which the outer loop is used to adjust the volume of materials and the inner loop is used to identify the optimal topology with minimum compliance. The ESM is an alternative method to solved performance-based topology optimization problems and provides a conservative solution for such problems in which only one functional constraint is active. The advantages of ESM are intuitive in concepts and easily programmed with the commercial FE software.

Our numerical examples demonstrate that the proposed ESM is a robust, stable, and efficient method to solve topology optimization problems with the volume constraint or functional constraints. For structures subjected to a single concentrated load with a displacement constraint, the optimal topologies produced by the ESM displayed the same trend as those by solving topology optimization with a volume constraint problems. The existence of displacement constraints controlled the final material volume according to the allowable displacement values. For structures with multiple displacement constraints, or in which the degree of freedom of the specified displacement constraint differs from that of the applied load, the final topologies varied locally with respect to the location of the active displacement constraints. The load pattern, to a large extent, determined the final optimal topology, while the displacement constraints mainly controlled the volume ratio.

ACKNOWLEDGEMENTS

The authors acknowledge the financial support of the Ministry of Science and Technology (MOST 104-2221-E-033-037), Republic of China (Taiwan). The authors also wish to acknowledge Simutech Solution Corporation for providing computational resources.

APPENDIX

The objective of topology optimization is to minimize the compliance of a structure, which can be written as follows:

$$\text{Min. } f(\mathbf{E}) = \mathbf{P}^T\mathbf{U} \tag{A1}$$

where $\mathbf{E}$ represents the set of design variables. In the switching stage, the elastic moduli of elements can be used as the design variables. The elements are assigned either the solid elastic modulus E_{solid} or a small value indicating the void elastic modulus E_{void}. In other words, the design variables are written as follows:

$$E_j = \begin{cases} E_{solid} \\ E_{void} \approx 0 \end{cases} \quad for\ j = 1, 2, \ldots, N_{ele} \tag{A2}$$

where N_{ele} denotes the number of elements in the finite element model. In addition, any topology of the structure in the design domain must satisfy the equilibrium equation as follows:

$$\mathbf{K}(\mathbf{E})\mathbf{U} = \mathbf{P} \tag{A3}$$

where $\mathbf{K}$ is the global stiffness matrix, which is a function of the set of design variables $\mathbf{E}$.

The objective function can be linearized about point $\mathbf{E}^*$, which represents a specific topology of the structure in the N_{ele}-dimensional space as follows:

$$f(\mathbf{E}) \approx \bar{f}(\mathbf{E}) = f(\mathbf{E}^*) + (\nabla f\big|_{\mathbf{E}=\mathbf{E}^*})^T(\mathbf{E} - \mathbf{E}^*) \tag{A4}$$

Eq. (A4) can be extended and rewritten as follows:

$$\begin{aligned} \bar{f}(\mathbf{E}) &= (\nabla f\big|_{\mathbf{E}=\mathbf{E}^*})^T\mathbf{E} - (\nabla f\big|_{\mathbf{E}=\mathbf{E}^*})^T\mathbf{E}^* + f(\mathbf{E}^*) \\ &= (\nabla f\big|_{\mathbf{E}=\mathbf{E}^*})^T\mathbf{E} + C \end{aligned} \tag{A5}$$

where C is a constant and can be ignored in the process of finding the minimum point of the linearized objective function.

On the other hand, differentiating Eq. (A3) with respect to the j^{th} design variable, for instance, E_j, gives the following:

$$\frac{\partial \mathbf{K}}{\partial E_j}\mathbf{U} + \mathbf{K}\frac{\partial \mathbf{U}}{\partial E_j} = \frac{\partial \mathbf{P}}{\partial E_j} \tag{A6}$$

Since the external force $\mathbf{P}$, in general, is not a function of E_j, Eq. (A6) can be rearranged as follows:

$$\frac{\partial \mathbf{U}}{\partial E_j} = -\mathbf{K}^{-1}\frac{\partial \mathbf{K}}{\partial E_j}\mathbf{U} \tag{A7}$$

The j^{th} component of the objection function gradient is as follows:

$$(\nabla f)_j = \frac{\partial f}{\partial E_j} = \left(\frac{\partial \mathbf{U}}{\partial E_j}\right)^T \mathbf{K}\mathbf{U} + \mathbf{U}^T\left(\frac{\partial \mathbf{K}}{\partial E_j}\right)\mathbf{U} + \mathbf{U}^T\mathbf{K}\left(\frac{\partial \mathbf{U}}{\partial E_j}\right) \tag{A8}$$

Substituting Eq. (A7) into Eq. (A8) and considering the symmetry of the global stiffness matrix, $\mathbf{K}$, one obtains the following:

$$(\nabla f)_j = \frac{\partial f}{\partial E_j} = -\mathbf{U}^T\left(\frac{\partial \mathbf{K}}{\partial E_j}\right)\mathbf{U} \tag{A9}$$

Since E_j appears only in the element stiffness matrix of the j^{th} element, differentiation of the global stiffness with respect to E_j gives nonzero matrix coefficients only if the coefficient corresponds to the stiffness matrix of the j^{th} element. In addition, the element stiffness matrix is proportional to E_j and the global displacement vector can be replaced by the nodal displacement vector of the j^{th} element in Eq. (A9). As a result, Eq. (A9) can be rewritten as follows:

$$(\nabla f)_j = \frac{\partial f}{\partial E_j} = -\mathbf{u}_j^T\left(\frac{\mathbf{k}_j}{E_j}\right)\mathbf{u}_j = -\frac{2w_j}{E_j} \tag{A10}$$

https://doi.org/10.1017/jmech.2017.68 Published online by Cambridge University Press

where $\mathbf{u}_j$ and $\mathbf{k}_j$ represent the nodal displacement vector and element stiffness matrix of the j^{th} element, respectively, and w_j denotes the strain energy of the j^{th} element.

Therefore, the linearized minimization problem is as follows:

$$\text{Min. } \bar{f}(\mathbf{E}) = -\sum_{j=1}^{N_{ele.}} \left(\frac{2w_j}{E_j} \right)\Bigg|_{\mathbf{E}=\mathbf{E}^*} E_j \tag{A11}$$

Furthermore, by introducing slack variables, the side constraints of the design variables can be written as follows [2]:

$$\begin{aligned} &E_1 + S_1 = E_{solid} \\ &E_2 + S_2 = E_{solid} \\ &\quad \vdots \\ &E_{N_{ele.}} + S_{N_{ele.}} = E_{solid} \end{aligned} \quad \text{with}$$

$$E_j, S_j \geq 0 \quad \text{for } j = 1, 2, \cdots, N_{ele} \tag{A12}$$

where S_j denotes the j^{th} slack variable. For instance, the j^{th} element is solid in an arbitrary topology, represented as $E_j = E_{solid}$ (basic variable) and $S_j = 0$ (non-basic variable). On the other hand, the j^{th} element is void in another arbitrary topology, represented as $E_j = E_{void} = 0$ (non-basic variable) and $S_j = E_{solid}$ (basic variable). Since all elements are either solid or void, Eq. (A11) can be rewritten in terms of basic variables as follows:

$$\begin{aligned} \text{Min. } \bar{f}(\mathbf{E}) &= -\sum_{j=1}^{N_{solid}} \left(\frac{2w_j}{E_j} \right)\Bigg|_{\mathbf{E}=\mathbf{E}^*} E_j - \sum_{j=1}^{N_{void}} \left(\frac{2w_j}{E_j} \right)\Bigg|_{\mathbf{E}=\mathbf{E}^*} (E_{solid} - S_j) \\ &= -\sum_{j=1}^{N_{solid}} \left(\frac{2w_j}{E_j} \right)\Bigg|_{\mathbf{E}=\mathbf{E}^*} E_j - E_{solid} \sum_{j=1}^{N_{void}} \left(\frac{2w_j}{E_j} \right)\Bigg|_{\mathbf{E}=\mathbf{E}^*} \\ &\quad + \sum_{j=1}^{N_{void}} \left(\frac{2w_j}{E_j} \right)\Bigg|_{\mathbf{E}=\mathbf{E}^*} S_j \end{aligned} \tag{A13}$$

where the second term of the right-hand side can be viewed as a constant.

To minimize the linearized objective function, the void element with the largest strain energy should be replaced by a solid element according to Eq. (A13). Similarly, the solid element with the lowest strain energy should be replaced by a void element, to reduce the increment in the linearized objective function. The element exchange process must be repeated until the largest strain energy of the void elements is less than the smallest strain energy of the solid elements. As a result, the element exchange in the sorting process of the switching stage is similar to the simplex method [27].

NOMENCLATURE

C_p Compliance of the structure;

M_r Number of elements exchanged at each iteration of the random switch;

$M_{r\text{-}max}$ Maximum number of elements exchanged at each iteration of the random switch;

$M_{r\text{-}min}$ Minimum number of elements exchanged at each iteration of the random switch;

M_s Number of elements exchanged at each iteration of the sorting switch;

$M_{s\text{-}max}$ Maximum number of elements exchanged at each iteration of the sorting switch;

$M_{s\text{-}min}$ Minimum number of elements exchanged at each iteration of the sorting switch;

$N_{s\text{-max}}$ Maximum iteration number;

R_V Volume adjustment parameter;

V Volume of the design domain;

V_s Solid volume of the structure;

$\mathbf{K}$ Global stiffness matrix;

$\mathbf{P}$ Global force vector;

$\mathbf{U}$ Global displacement vector;

$\mathbf{u}$ nodal displacement vector;

REFERENCES

1. Rozvany, G. I. N., "Layout Theory for Grid-Type Structures," *Topology Design of Structures,* Kluwer Academic Publishers, London, pp. 251-272 (1993).
2. Tanskanen, P., "The Evolutionary Structural Optimization Method: Theoretical Aspects," *Computer Methods in Applied Mechanics and Engineering*, **191**, pp. 5485-5498 (2002).
3. Bendsøe, M. P. and Kikuchi, N., "Generating Optimal Topologies in Structural Design Using a Homogenization Method," *Computer Methods in Applied Mechanics and Engineering*, **71**, pp. 197-224 (1988).
4. Suzuki, K. and Kikuchi, N., "A Homogenization Method for Shape and Topology Optimization," *Computer Methods in Applied Mechanics and Engineering*, **93**, pp. 291-318 (1991).
5. Bendsøe, M. P., "Optimal Shape Design as a Material Distribution Problem," *Structural Optimization*, **1**, pp. 193-202 (1989).
6. Mlejnek, H. P., "Some Aspects of the Genesis of Structures," *Structural Optimization*, **5**, pp. 49-64 (1992).
7. Bendsøe, M. P., *Optimization of Structural Topology, Shape and Material*, Springer, Berlin (1995).
8. Baumgartner, A., Harzheim, L. and Mattheck, C., "SKO (Soft Kill Option): the Biological Way to Find an Optimum Structure Topology," *Internation-*

https://doi.org/10.1017/jmech.2017.68 Published online by Cambridge University Press

al Journal of Fatigue, **14**, pp. 387-393 (1992).

9. Xie, Y. M. and Steven, G. P., "A Simple Evolutionary Procedure for Structural Optimization," *Computers and Structures*, **49**, pp. 885-896 (1993).
10. Yang, X. Y., Xie, Y. M., Steven, G. P. and Querin, Q. M., "Bidirectional Evolutionary Method for Stiffness Optimization," *AIAA Journal*, **37**, pp. 1483- 1488 (1999).
11. Huang X. and Xie, Y. M., "Bi-Directional Evolutionary Topology Optimization of Continuum Structure with One or Multiple Material," *Computational Mechanics*, **43**, pp. 393-401 (2009).
12. Rouhi, M., Rais-Rohani, M. and Williams, T. N., "Element Exchange Method for Topology Optimization," *Structural and Multidisciplinary Optimization*, **42**, pp. 215-231 (2010).
13. Wang, M. Y., Wang, X. and Guo, D., "A Level Set Method for Structural Topology Optimization," *Computer Methods in Applied Mechanics and Engineering*, **192**, pp. 227-246 (2003).
14. Mei, Y. L. and Wang, X. M., "A Level Set Method for Structural Topology Optimization and Its Applications," *Advances in Engineering software*, **35**, pp. 415-441 (2004).
15. Amstutz, S. and Andrä, H., "A New Algorithm for Topology Optimization Using a Level-Set Method," *Journal of Computational Physics*, **216**, pp. 573-588 (2006).
16. Chu, D. N., Xie, Y. M., Hira, A. and Steven, G. P., "Evolutionary Structural Optimization for Problems with Stiffness Constraints," *Finite Element in Analysis and Design*, **21**, pp. 239-251 (1996).
17. Chu, D. N., Xie, Y. M., Hira, A. and Steven, G. P., "On Various Aspects of Evolutionary Structural Optimization for Problems with Stiffness Constraints," *Finite Element in Analysis and Design*, **24**, pp. 197-212 (1997).
18. Zhao, C., Steven, G. P. and Xie, Y. M., "Evolutionary Natural Frequency Optimization of Thin Plate Bending Vibration Problems," *Structural Optimization,* **11**, pp. 244-251 (1996).
19. Bendsøe, M. P. and Sigmund, O. *Topology Optimization: Theory, Methods, and Applications*, Springer, Berlin (2003).
20. Huang, X. and Xie, Y. M., "Evolutionary Topology Optimization of Continuum Structure with an Additional Displacement Constraint," *Structural and Multidisciplinary Optimization*, **40**, pp. 409-416 (2010).
21. Lin, C. Y. and Hsu, F. M., "An Adaptive Volume Constraint Algorithm for Topology Optimization with a Displacement-limit," *Advances in Engineering Software*, **39**, pp. 973-994 (2008).
22. Lin, C. Y. and Hsu, F. M., "Adaptive Volume Constraint Algorithm for Stress Limit-Based Topology Optimization," *Computer-Aided Design*, **41**, pp. 685-694 (2009).
23. Li, Q., Steven, G. P. and Xie, Y. M., "A Simple Checkerboard Suppression Algorithm for Evolutionary Structural Optimization," *Structural and Multidisciplinary Optimization*, **22**, pp. 230-239 (2001).
24. *Abaqus User's Manual*, Dassault Systèmes Simulia (2016).
25. Zuo, Z. H. and Xie, Y. M., "A Simple and Compact Python Code for Complex 3D Topology Optimization," *Advances in Engineering Software*, **85**, pp. 1-11 (2015).
26. Huang, X. and Xie, Y. M., "A Further Review of ESO Type Methods for Topology Optimization," *Structural and Multidisciplinary Optimization*, **41**, pp. 671-683 (2010).
27. Arora, J. S., *Introduction to Optimum Design*, 3rd edit., Academic Press, Boston (2011).

(Manuscript received October 25, 2016,
accepted for publication June 23, 2017.)

https://doi.org/10.1017/jmech.2017.68 Published online by Cambridge University Press